Geophysical Research Letters

RESEARCH LETTER
10.1029/2019GL083999

Submesoscale and Mesoscale Eddies in the Florida Straits: Observations from Satellite Ocean Color Measurements

Yingjun Zhang[1], Chuanmin Hu[1], Yonggang Liu[1], Robert H. Weisberg[1], and Vassiliki H. Kourafalou[2]

[1]College of Marine Science, University of South Florida, St. Petersburg, FL, USA, [2]Rosenstiel School of Marine and Atmospheric Science, University of Miami, Miami, FL, USA

Key Points:
- Novel satellite imagery enable detection and characterization of submesoscale eddies
- The size of submesoscale eddies (radius of 2-15 km) in the Florida Straits tends to show a normal distribution
- There appears an increasing trend in submesoscale eddy occurrence in the Upper Keys of the Florida straits between 2002-2018

Supporting Information:
- Supporting Information S1

Correspondence to:
C. Hu,
huc@usf.edu

Citation:
Zhang, Y., Hu, C., Liu, Y., Weisberg, R. H., & Kourafalou, V. H. (2019). Submesoscale and mesoscale eddies in the Florida straits: observations from satellite ocean color measurements. *Geophysical Research Letters*, *46*, 13,262–13,270. https://doi.org/10.1029/2019GL083999

Received 4 JUN 2019
Accepted 18 NOV 2019
Accepted article online 20 NOV 2019
Published online 29 NOV 2019

Abstract Despite their well-recognized importance in driving ocean physics and biology, submesoscale (diameter < Rossby radius of deformation) eddies have been extremely difficult to observe due to technical difficulties from both field and remote platforms. Here using novel satellite ocean color data products and modified algorithms, we address this challenge for the Florida Straits (22–28°N, 78–85°W). Between 2002 and 2018, while mesoscale eddies (radius >15 km) show strong seasonality with occurrence frequency decreasing from Lower Keys to Upper Keys, submesoscale eddies show little or no seasonality with high occurrence frequency restricted to 30–200-m isobaths. The number of mesoscale eddies decreases exponentially in size, but submesoscale eddies show a normal distribution in size. These findings are significant in filling our knowledge gap in submesoscale eddies in this physically and ecologically important region as it encompasses world-renowned coral reefs, seagrasses, and fisheries.

1. Introduction

Submesoscale eddies can efficiently transport heat and salt in the upper ocean (Wang et al., 2018) and play an important role in the balance of energy generation and dissipation of larger scale oceanic processes (Munk et al., 2000; Zatsepin et al., 2019). However, compared to mesoscale eddies, they remain poorly studied due to technical difficulties in observing these small-scale and ephemeral ocean features. Satellite altimeters typically cannot characterize eddies smaller than 100–200 km in diameter. In subtropical and tropical oceans sea surface temperature imagery lose their spatial contrast during summer, and satellite ocean color imagery also suffer to lack of sufficient observations due to clouds, strong sun glint, and stray light (Chen et al., 2019; Hu, 2011). As a result, to date, there is generally a lack of synoptic and long-term characterization of submesoscale eddies in the world's oceans, except perhaps in some small regions when continuous land-based *h*igh frequency-radar observations are available.

The lack of observations also leads to a poor understanding on how these submesoscale features may affect local nutrient transport, biology, and ecology. This problem is particularly significant for the Florida Straits (FS), a subtropical region hosting the largest reef system in the continental United States and rich in submesoscale eddies as revealed by field surveys (Chew, 1974; ; de Morais & Reinert, 2010; Fiechter et al., 2008; Lee, 1975; Haus et al., 2000, 2004; Lee & Atkinson, 1983; Lee et al., 1995; Scott et al., 2010Shulzitski et al., 2017). Here submesoscale eddies refer to those with diameters less than a baroclinic Rossby radius of deformation (about 30 km; He & Weisberg, 2003; de Morais & Reinert, 2010; Kourafalou & Kang, 2012; Shay et al., 2007). The cyclonic eddies in this region are known to be highly productive with abundant nutrients, phytoplankton, and copepods (Hitchcock et al., 2005; Lee et al., 1994). These eddies have also been connected to the transport of biochemical substances from the deep ocean to the shallow coastal reef environments; these include fish larvae, nutrients, and pollutants (Kourafalou & Kang, 2012; Lane et al., 2003; Lee et al., 1992; Limouzy-Paris et al., 1997Sponaugle et al., 2005; Shulzitski et al., 2017). However, nearly all these studies are based on limited ship or *high frequency*-radar measurements, which lack spatial and temporal coverage. Therefore, the objective of this study is to use modified methods and novel data products to establish a complete data record of eddy occurrence in the FS and then understand their spatial/temporal changes as well as their possible long-term trends.

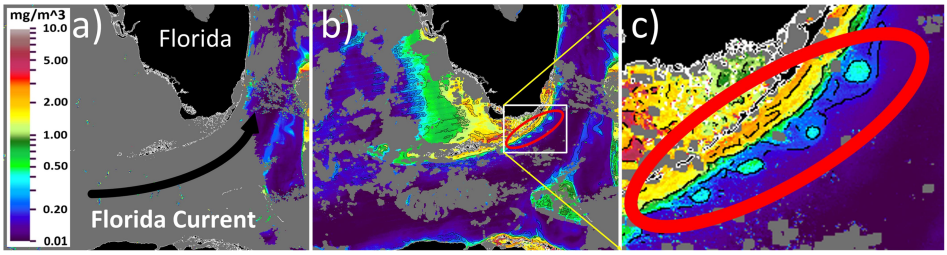

Figure 1. Demonstration of eddy extraction from MODIS/A Chl images over the Florida Straits on 29 June 2004. (a) Standard NASA Chl image does not have sufficient coverage due to sun glint and stray light; (b) New Chl image after data "recovering" (Chen et al., 2019; Hu, 2011); The images cover a region of 23°N to 27°N and 84°W to 79°W. A small portion outlined by the rectangular box is enlarged in (c), where submesoscale cyclonic eddy features are delineated in black using the techniques developed in this study.

2. Data and Method

2.1. Data

The fundamental difficulty of lacking appropriate data product in systematically characterizing submesoscale features is overcome in this study through the use of novel ocean color algorithms and data products. Specifically, sun glint and stray light are corrected through an empirically color index algorithm (Hu, 2011). Then, a machine learning approach is used to "recover" these corrected but low-quality data to chlorophyll (Chl in mg m^{-3}) data, whose quality is comparable to the NASA standard Chl data product (Chen et al., 2019). This way, without losing quality, Chl data quantity can be increased by 3–5 times, especially during summer time.

In this study, data collected by the Moderate Resolution Imaging Spectroradiometer (MODIS) onboard the Aqua satellite were obtained from the NASA Goddard Space Flight Center (https://oceancolor.gsfc.nasa.gov). The daily data covered a period of July 2002–April 2018. Using the approaches outlined in Hu (2011) and Chen et al. (2019), novel Chl data products were derived. These data products are generally immune to perturbations by sun glint, thin clouds, stray light, and sensor saturation, therefore providing significantly improved coverage in both space and time in all four seasons and making this study possible. Figures 1a and 1b show the contrast between the standard NASA Chl and the new Chl, where the latter reveals several submesoscale eddies along the Florida Keys. Because MODIS land bands were used to derive the new Chl data products (to avoid the sensor saturation problem), these data products have a nominal resolution of 500 m, sufficient to characterize submesoscale features.

2.2. Method

While several approaches have been proposed in the past to delineate ocean fronts and eddy boundaries, the Canny edge detection algorithm (Canny, 1986) was selected in this study because it is relatively easy to implement to apply to sea surface temperature and ocean color imagery, and previous studies (Castelao et al., 2006; Castelao & Wang, 2014; Wall et al., 2008; Wang et al., 2015) proved its effectiveness in delineating ocean fronts. Therefore, a modified Canny method was used to delineate the eddy boundaries using the following steps.

The algorithm used to delineate eddy boundaries in this study consisted in the following steps:

1. Pixels within 2 km of land or clouds are discarded, as these pixels may be contaminated by stray light.
2. A Gaussian filter was used to remove image noise. The standard deviation of the Gaussian filter, sigma, was selected to be 2.0 (corresponding to a 13×13 pixel window) in order to achieve the best eddy boundary delineation results.
3. The gradient for each pixel was computed by applying a Sobel gradient operator towards the smoothed image.
4. Non-maximum suppression was applied to the gradient image to "thin" the spatially thick boundaries.
5. Two thresholds, 0.02 and 0.09 mg/m^3 per 100 km, were applied to determine the candidate boundaries for eddy detection. The threshold values were determined after trial-and-error analyses of 625 sets of threshold values to determine which set was optimal for front detection (as judged by the gradient

images). The connected boundary pixels with spatial gradients below the lower threshold were removed, while the connected boundary pixels with spatial gradients above the upper threshold were retained. For candidate boundaries whose pixel gradients were between the two thresholds, only when these pixels were connected to the boundary pixels with spatial gradient above the upper threshold were they retained. This step was followed through an edge tracking algorithm.

6. For the selected boundaries, those closed in space were determined to form an eddy.

After delineation of eddy boundaries, an equivalent eddy radius was defined as the radius of a circle with the same area as the delineated eddy, and pixels within the boundaries were considered as "eddy pixels." Then, for each pixel in the image, eddy occurrence frequency was calculated as $f = \mathrm{N/C} \times 100\%$, where N is the number of times during the observation period that the pixel is an eddy pixel, and C is the number of times the pixel could be judged to be either an eddy pixel or a non-eddy pixel.

Six transects were selected around the Dry Tortugas, Marquesas Keys, Lower Keys, Middle Keys, Upper Keys, and Miami. Each transect starts from 30-m isobaths, with the lengths of first two transects being about 130 km and of other four transects being about 45 km.

In each image, the number of eddies was determined using a Matlab program developed in house after delineation of eddy boundaries. Here the focus is on cyclonic eddies, where Chl is higher within the eddy than outside the eddy. It is unknown whether there are anticyclonic eddies from ocean color imagery because of lack of spatial contrast.

To determine the Florida Current (FC) positions, we used the Archiving, Validation and Interpretation of Satellite Oceanographic Data (AVISO+) multi-mission gridded sea level anomaly data distributed by the Copernicus Marine Environment Monitoring Service. Surface geostrophic current velocities were derived following a procedure described in Liu et al. (2016), and the currents were further interpolated onto the transects. A threshold of 0.5 m/s of geostrophic current speed was used to indicate the northern edge of the FC on a transect, similar to that for the eastern boundary of the Loop Current system approaching the Dry Tortugas area (Weisberg & Liu, 2017).

To determine whether the eddy occurrence frequency is related to the FC position in different seasons, a correlation analysis was performed for each season between these two parameters. The same correlation analysis was also performed when the time series data were treated as a whole without being partitioned into seasons. In this case, the seasonality was removed by subtracting the long-term monthly climatology.

3. Results

Figure 1 shows that while the NASA standard Chl image is significantly blocked by sun glint and cloud-adjacent stray light (Figure 1a), the new Chl image is immune to these perturbations (Figure 1b), thus revealing the submesoscale features along the Florida Keys. Furthermore, using the eddy delineation method described above, the boundaries of these submesoscale eddies are outlined in black (Figure 1c). More cases showing the contrast between the NASA standard Chl and new Chl images can be seen from Figure S1 in the supporting information. The number of eddies, their sizes, and whether a pixel falls within the boundary are all recorded from the boundary lines, and this process is repeated for all images between 2002 and 2018 to generate eddy occurrence statistics, as shown in Figures 2–4.

The frequency of mesoscale eddy occurrence in the four climatological seasons of 2002–2018 is shown in Figures 2a–2d. More eddies are observed in summer, followed by fall and spring, with the lowest occurrence in winter. The occurrence frequency decreases gradually from the Lower Keys to the Upper Keys, with the highest occurrence frequency occurring around the Dry Tortugas.

The frequency of submesoscale eddy occurrence in the four climatological seasons of 2002–2018 is shown in Figures 2e–2h. More eddies are observed in the coastal regions of 26°N to 27°N, where summer appears to have more submesoscale eddies than any other seasons. The high occurrence region is bounded approximately by 30 and 200-m isobaths, while the Miami region appears to have higher occurrence frequency than other regions.

These observations can be well explained from the perspective of ocean hydrodynamics. Previous studies (Fratantoni et al., 1998; Lee et al., 1994; Sponaugle et al., 2005) have discussed the evolution of cyclonic

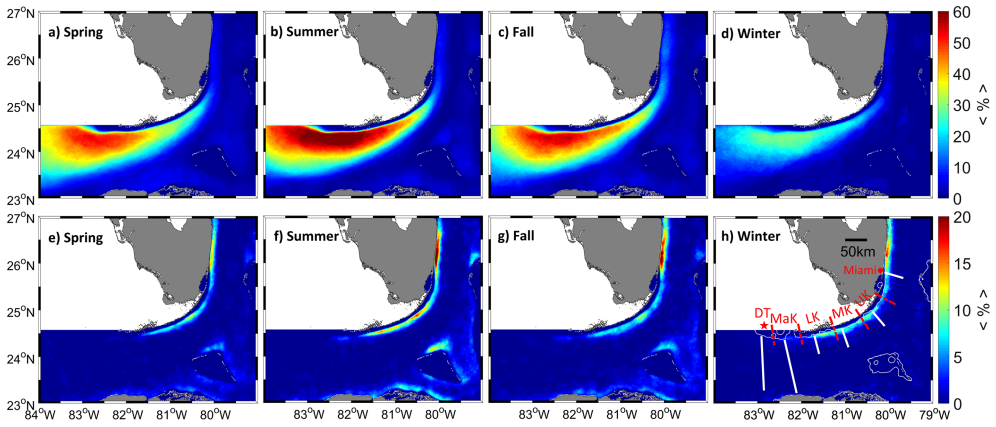

Figure 2. Distribution of occurrence frequency of mesoscale (a–d) and submesoscale (e–h) eddies in the Florida Straits during four climatological seasons between 2002 and 2018. Color codes indicate percentage of images where a location is within an eddy. In (h), six cross-strait transects are annotated with thick white lines, along which time series of eddy occurrence are presented in Figure 3. 30-m isobaths are annotated with thin white lines. The dashed red lines in (h) denote Florida Keys subdomains: MaK: Marquesas Keys, LK: Lower Keys, MK: Middle Keys, UK: Upper Keys; DT: Dry Tortugas is marked with a red pentagram, and Miami is marked with a red dot.

eddies from the broader western entrance of the FS near the Dry Tortugas to the northern part of the Upper Keys region. Due to the interaction between the Florida Current and the topography, eddies change in size and propagating speed (Kourafalou et al., 2009; Lee et al., 1995; Sponaugle et al., 2005). They may also transform, splitting into smaller (submesoscale) eddies, while formation of additional cyclonic eddies can also take place locally (Kourafalou & Kang, 2012).

Figures 3a and 3b show mesoscale eddy occurrence frequency along the first two cross-strait transects, where the position of the FC is overlaid with black lines. Figures 3c–3f present submesoscale eddy occurrence frequency along the other four cross-strait transects. To examine their potential relationship with the FC's position, Figure 3e is repeated in Figure 3g but with the position of the FC overlaid with black lines.

While the spatial distributions of eddy occurrence are revealed in the eddy occurrence frequency maps in Figure 2, the temporal changes of eddies along the six cross-strait transects (Figure 2d) are shown in Figure 3. Similar to those in Figures 2, 3a, and 3b show significant seasonality in mesoscale eddy occurrence. The results of wavelet analysis (Liu et al., 2007) of the outlined region in Figure S2a on mesoscale eddy occurrence frequency, which can be seen from Figure S3b, also support this conclusion. Wavelet power spectra of mesoscale eddy occurrence frequency are statistically significant at a 12-month period (note the annotated horizontal red dashed line in Figure S3b), which indicates consistent annual cycle (seasonal variation) of mesoscale eddy occurrence. For Transect 1 (Dry Tortugas) and Transect 2 (Marquesas), the highest frequency occurs in the summer of every year except 2012. During the summer months, the occurrence frequency of mesoscale eddies is highly correlated with the position of the FC, with their correlation coefficients ranging between 0.78 and 0.54 for Transect 1 (Dry Tortugas) and Transect 2 (Marquesas), respectively. In addition, there appears an increasing trend in occurrence frequency of mesoscale eddies (Figures 3a and 3b). However, because this may be the result of more stationary eddies in certain years (e.g., 2017), it is currently unclear whether this trend is a result of increased number of eddies or more stationary eddies in certain years. Determining unique eddies requires tracking individual eddies, which is currently difficult or impossible due to frequent cloud cover in ocean color imagery, but might be possible in the future when combining observations with numerical models. In contrast, the increasing trends of occurrence frequency of submesoscale eddies in the Upper Keys (Figure 3e) and along Transect 6 (Miami, Figure 3f, more eddies in 2015–2018 than in earlier years) are likely realistic as submesoscale cyclonic eddies moved much faster than mesoscale cyclonic eddies. For submesoscale eddies along the other four transects, their seasonality in occurrence frequency is much weaker than that for mesoscale eddies. Although summer months appear to have higher occurrence frequency visually, wavelet power spectra of the outlined region in Figure S2b for submesoscale eddy occurrence frequency (Figure S3d) show eddy energy mainly in short

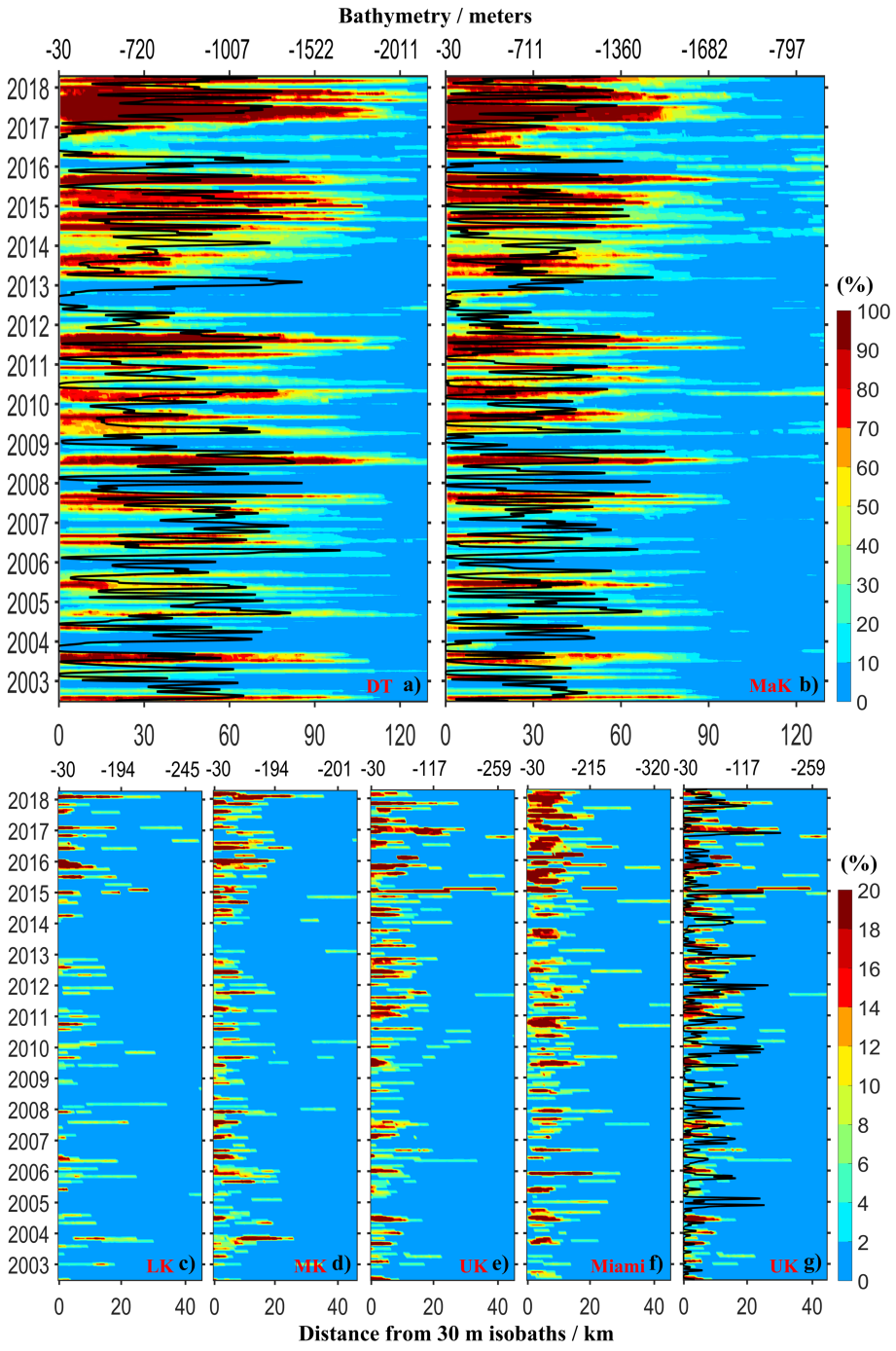

Figure 3. Time series of eddy occurrence frequency along the six cross-strait transects (a–f), shown in Figure 2h. Labels on the bottom indicate distance from the 30-m isobaths, while labels on the top show bathymetry. The year mark starts from January of that year. The position of the Florida Current is annotated as black lines in Figures 3a and 3b. Figure 3g is the same as Figure 3e but with the blackline overlaid.

frequency band with periods of 2–10 months. In contrast to mesoscale eddies, the occurrence frequency of submesoscale eddies does not appear to correlate well with the position of the FC (Figure 3g): the correlation coefficient for Transect 5 (Upper Keys) for summer months is only 0.36, which decreases to 0.025 when all months (except winter months) are considered.

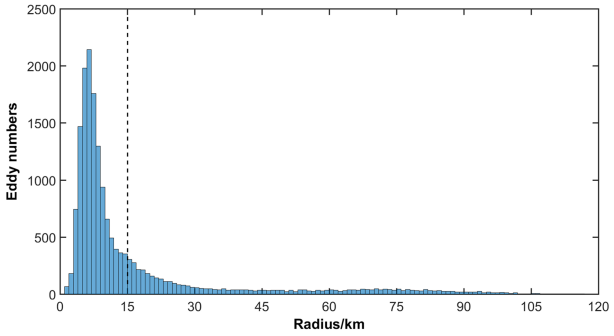

Figure 4. Histogram of number of cyclonic mesoscale and submesoscale eddies in the Florida Straits observed from all MODIS images between 2002 and 2018. The dashed vertical line denotes the separation of submesoscale (radius <15 km) and mesoscale eddies.

A total of 6,140 images were used in this study (of which 2,046 images were mostly cloud-free) to estimate the number of eddies. Figure 4 shows the number of cyclonic mesoscale and submesoscale eddies observed between 2002 and 2018 for each eddy size. Most of the observed eddies are small, with 84% of them being submesoscale (radius <15 km, dashed line in Figure 4). Within this group, most eddies are found with a radius of 6–7 km. While the distribution of submesoscale eddies appears to be normal, the number of mesoscale eddies decreases exponentially with eddy size. This observation is consistent with results obtained from a numerical model for the Southern California Bight (Dong et al., 2012). Note that nearly all eddies observed have radius <100 km. Clearly, if satellite altimetry was to be used to study eddies, most of them would be missed completely.

The new Chl images not only made it possible to derive eddy statistics (as shown in Figures 2–4) but were also used to estimate the eddy's moving speed when sequential images (e.g., Figures S4 and S5) showing the same eddies were available. Mesoscale eddies that formed off the Dry Tortugas moved relatively slowly at an averaging speed of 5–6 km/day, whereas FC frontal eddies (mesoscale eddies that did not form off the Dry Tortugas or submesoscale eddies) were observed to move quickly at speeds of 20 to 35 km/day. These observations are comparable to those obtained from field measurements or numerical models (Lee et al., 1995; Limouzy-Paris et al., 1997; Shay et al., 1998; Parks et al., 2009; Kourafalou & Kang (2012)).

4. Discussion

4.1. Uncertainties

Due to the ephemeral nature of submesoscale eddies, direct field validation of the above eddy statistics is impossible. High-resolution numerical models may provide independent data to qualitatively validate these results. For example, Kourafalou and Kang (2012) used a 1/100° HYCOM model to estimate the number of cyclonic mesoscale and submesoscale eddies in each of the subdomains in Figure 2h over the period of 2004–2008. They found that there was an increase in submesoscale vortices from the Dry Tortugas to the upper part of the Upper Keys, but the number of mesoscale vortices was generally reduced, because they either sheared apart or split to smaller eddies. These modeling results are in line with the observations based on ocean color imagery here, thus supporting the validity of the observations in a qualitative way. Furthermore, a sensitivity test indicates that the eddy statistics were relatively stable against changes in algorithm parameterization (Figure S6), suggesting that the results presented here are at least self-consistent. In the future, *high frequency*-radar data may be used to study individual cases to result in direct validations.

4.2. Seasonal and Interannual Changes

Seasonal variability of ocean circulation is complicated in this region. To the west, the Gulf of Mexico Loop Current system does not appear to have seasonal variations. In the Loop Current active region, the variability is dominated by intra-seasonal frequency band (Liu et al., 2016). In the Straits of Florida, the transport has semi-annual cycles with a larger value in summer, which can be largely explained by along-channel winds (Rousset & Beal, 2011). The winds in the Florida Keys region have seasonal variation, southeast in summer and northeast in winter (Liu & Weisberg, 2012). It is not intuitive how the winds and the FC affect the mesoscale and submesoscale eddies.

The interannual changes of mesoscale eddy occurrence frequency are correlated with changes in the position of the FC. However, occurrence frequency of submesoscale eddies does not show the same correlation even though submesoscale eddies can occur anywhere along the frontal boundary as mesoscale eddies decay or as the FC meanders along the shelf edge (Lee, 1975). Multiple processes may be involved in forming the submesoscale eddies.

4.3. Implications

While the mechanisms behind the spatial and temporal changes of both mesoscale and submesoscale eddies are derived mainly from previous research and from educated speculations, there is consensus on

the implication from the rotating currents within these vortices. These currents influence the shallow areas of the Reef Tract, and they can retain materials, such as fish larvae. This is a mechanism of retaining material and, in the case of fish larvae, biological processes such as recruitment and connectivity can be affected. In particular, spawning grounds in the Dry Tortugas can provide larvae that will travel with the cyclonic eddies and reach downstream reefs, an important connectivity pathway. (Kourafalou et al., 2018; Lee et al., 1992, 1994; Limouzy-Paris et al., 1997; Lee & Williams, 1999; Sponaugle et al., 2005; Shulzitski et al., 2015, 2016; Vaz et al., 2016). Submesoscale cyclonic eddies can also provide a favorable feeding environment for sailfish larvae and potentially also for their adults (Richardson et al., 2009). Therefore, the information obtained from this study provides more insight to the complex near-surface circulation systems and important implications for nutrient flux, biological productivity, plankton patchiness, larval transport and recruitment, and dispersal of pollutants. The eddy occurrence frequency maps presented in this study may therefore provide some guidance in the future when designing field sampling plans. In particular, the near real-time availability of the novel ocean color imagery enables tracking of individual eddies in sequential images (see Supporting information), thus making it possible to follow individual eddies through ship surveys.

The study region is ecologically important but relatively small. However, the approach presented here may serve as a template for many other regions in order to map mesoscale and submesoscale eddies and understand their roles in affecting physical transport of materials and local biogeochemistry. Figure S7 shows such an example, where a submesoscale eddy in the western Gulf of Mexico is detected from the novel MODIS/A Chl image on 10 June 2018.

In a broader sense, this study represents a pioneering effort in characterizing submesoscale eddies well in advance of the U.S. NASA's Surface Water and Ocean Topography (SWOT) mission (https://swot.jpl.nasa.gov/) and particularly in providing possible solutions to fill some of the SWOT temporal and spatial gaps. This is because the 15-km resolution SWOT mission has a temporal resolution of ~10–20 days, while the novel Chl product can detect submesoscale eddies of ~5–10 km every 4–5 days as long as these eddies have a color contrast.

5. Conclusions

Submesoscale eddies have been difficult to characterize in a systematic fashion because of their ephemeral nature and lack of observing techniques. In this study, we show that a modified Canny edge detection algorithm applied to a novel ocean color data product can map both mesoscale and submesoscale eddies in the Florida Straits, from which long-term eddy distribution patterns between 2002 and 2018 can be derived. We believe that this is the first time such eddies are documented from systematic observations. Results show unprecedented information on their seasonality and interannual changes, while the availability of ocean color data globally makes extension of the current study to other coastal regions straightforward.

Acknowledgments
This work was supported by the U.S. National Aeronautics and Space Administration (NNX14AL98G), National Oceanic and Atmospheric Administration (NA15OAR4320064), Gulf of Mexico Research Initiative (GOMA231607-00, G-231804 and G-231819), and National Academies of Sciences, Engineering and Medicine (UGOS, 2000009918), and by a NASA student fellowship (FINESST, 80NSSC19K1358). All images can be found and accessed at the Gulf of Mexico Research Initiative Information and Data Cooperative (GRIIDC) at https://data.gulfresearchinitiative.org/pelagos-symfony/data/R6.x818.000:0001 (doi: 10.7266/n7-adrz-4567). We thank Dr. Igor Belkin (University of Rhode Island) for the useful discussions on the various edge detection methods applied to satellite imagery. We thank Mr. Brock Murch (USF) for his various editorial comments, and thank the two anonymous reviewers for their contribution in improving the presentation of this work.

References

Canny, J. (1986). A computational approach to edge detection. *IEEE Transactions on Pattern Analysis and Machine Intelligence*, *6*, 679–698.

Castelao, R. M., Mavor, T. P., Barth, J. A., & Breaker, L. C. (2006). Sea surface temperature fronts in the California Current System from geostationary satellite observations. *Journal of Geophysical Research*, *111*, C09026. https://doi.org/10.1029/2006JC003541

Castelao, R. M., & Wang, Y. (2014). Wind-driven variability in sea surface temperature front distribution in the California Current System. *Journal of Geophysical Research: Oceans*, *119*, 1861–1875. https://doi.org/10.1002/2013JC009531

Chen, S., Hu, C., Barnes, B. B., Xie, Y., Lin, G., & Qiu, Z. (2019). Improving ocean color data coverage through machine learning. *Remote Sensing of Environment*, *222*, 286–302. https://doi.org/10.1016/j.rse.2018.12.023

Chew, F. (1974). The turning process in meandering currents: A case study. *Journal of Physical Oceanography*, *4*(1), 27–57. https://doi.org/10.1175/1520-0485(1974)004<0027:TTPIMC>2.0.CO;2

de Morais, B., & Reinert, C. (2010). On the evolution of cyclonic eddies along the Florida Keys (Master's thesis, University of Miami, Coral Gables, Florida). https://scholarlyrepository.miami.edu/cgi/viewcontent.cgi?article=1069&context=oa_theses.

Dong, C., Lin, X., Liu, Y., Nencioli, F., Chao, Y., Guan, Y., et al. (2012). Three-dimensional oceanic eddy analysis in the Southern California Bight from a numerical product. *Journal of Geophysical Research*, *117*, C00H14. https://doi.org/10.1029/2011JC007354

Fiechter, J., Haus, B. K., Melo, N., & Mooers, C. N. (2008). Physical processes impacting passive particle dispersal in the Upper Florida Keys. *Continental Shelf Research*, *28*(10-11), 1261–1272. https://doi.org/10.1016/j.csr.2008.02.018

Fratantoni, P. S., Lee, T. N., Podesta, G. P., & Muller-Karger, F. (1998). The influence of Loop Current perturbations on the formation and evolution of Tortugas eddies in the southern Straits of Florida. *Journal of Geophysical Research*, *103*(C11), 24,759–24,779. https://doi.org/10.1029/98JC02147

Haus, B. K., Wang, J. D., Martinez-Pedraja, J., & Smith, N. (2004). Southeast Florida Shelf circulation and volume exchange, observations of km-scale variability. *Estuarine, Coastal and Shelf Science*, *59*(2), 277–294. https://doi.org/10.1016/j.ecss.2003.09.009

Haus, B. K., Wang, J. D., Rivera, J., Martinez-Pedraja, J., & Smith, N. (2000). Remote radar measurement of shelf currents off Key Largo, Florida, USA. *Estuarine, Coastal and Shelf Science*, *51*(5), 553–569. https://doi.org/10.1006/ecss.2000.0704

He, R., & Weisberg, R. H. (2003). A Loop Current intrusion case study on the West Florida Shelf. *Journal of Physical Oceanography*, *33*(2), 465–477. https://doi.org/10.1175/1520-0485(2003)033<0465:ALCICS>2.0.CO;2

Hitchcock, G. L., Lee, T. N., Ortner, P. B., Cummings, S., Kelble, C., & Williams, E. (2005). Property fields in a Tortugas Eddy in the southern straits of Florida. *Deep Sea Research Part I: Oceanographic Research Papers*, *52*(12), 2195–2213. https://doi.org/10.1016/j.dsr.2005.08.006

Hu, C. (2011). An empirical approach to derive MODIS ocean color patterns under severe sun glint. *Geophysical Research Letters*, *38*, L01603. https://doi.org/10.1029/2010GL045422

Kourafalou, V. H., Androulidakis, Y. S., Kang, H., Smith, R. H., & Valle-Levinson, A. (2018). Physical connectivity between Pulley Ridge and Dry Tortugas coral reefs under the influence of the Loop Current/Florida Current system. *Progress in Oceanography*, *165*, 75–99. https://doi.org/10.1016/j.pocean.2018.05.004

Kourafalou, V. H., & Kang, H. (2012). Florida Current meandering and evolution of cyclonic eddies along the Florida Keys Reef Tract: Are they interconnected? *Journal of Geophysical Research*, *117*, C05028. https://doi.org/10.1029/2011JC007383

Kourafalou, V. H., Peng, G., Kang, H., Hogan, P. J., Smedstad, O. M., & Weisberg, R. H. (2009). Evaluation of global ocean data assimilation experiment products on South Florida nested simulations with the Hybrid Coordinate Ocean Model. *Ocean Dynamics*, *59*(1), 47–66. https://doi.org/10.1007/s10236-008-0160-7

Lane, P. V., Smith, S. L., Graber, H. C., & Hitchcock, G. L. (2003). Mesoscale circulation and the surface distribution of copepods near the south Florida Keys. *Bulletin of Marine Science*, *72*(1), 1–18.

Lee, T. N. (1975, November). Florida Current spin-off eddies. *Deep Sea Research and Oceanographic Abstracts*, *22*(11), 753–765. https://doi.org/10.1016/0011-7471(75)90080-7

Lee, T. N., & Atkinson, L. P. (1983). Low-frequency current and temperature variability from Gulf Stream frontal eddies and atmospheric forcing along the southeast U.S. outer continental shelf. *Journal of Geophysical Research*, *88*(C8), 4541–4567. https://doi.org/10.1029/JC088iC08p04541

Lee, T. N., Clarke, M. E., Williams, E., Szmant, A. F., & Berger, T. (1994). Evolution of the Tortugas Gyre and its influence on recruitment in the Florida Keys. *Bulletin of Marine Science*, *54*(3), 621–646.

Lee, T. N., Leaman, K., Williams, E., Berger, T., & Atkinson, L. (1995). Florida Current meanders and gyre formation in the southern Straits of Florida. *Journal of Geophysical Research*, *100*(C5), 8607–8620. https://doi.org/10.1029/94JC02795

Lee, T. N., Rooth, C., Williams, E., McGowan, M., Szmant, A. F., & Clarke, M. E. (1992). Influence of Florida Current, gyres and wind-driven circulation on transport of larvae and recruitment in the Florida Keys coral reefs. *Continental Shelf Research*, *12*(7-8), 971–1002. https://doi.org/10.1016/0278-4343(92)90055-O

Lee, T. N., & Williams, E. (1999). Mean distribution and seasonal variability of coastal currents and temperature in the Florida Keys with implications for larval recruitment. *Bulletin of Marine Science*, *64*(1), 35–56.

Limouzy-Paris, C. B., Graber, H. C., Jones, D. L., Röpke, A. W., & Richards, W. J. (1997). Translocation of larval coral reef fishes via sub-mesoscale spin-off eddies from the Florida Current. *Bulletin of Marine Science*, *60*(3), 966–983.

Liu, Y., Liang, X. S., & Weisberg, R. H. (2007). Rectification of the bias in the wavelet power spectrum. *Journal of Atmospheric and Oceanic Technology*, *24*(12), 2093–2102. https://doi.org/10.1175/2007JTECHO511.1

Liu, Y., & Weisberg, R. H. (2012). Seasonal variability on the West Florida Shelf. *Progress in Oceanography*, *104*, 80–98. https://doi.org/10.1016/j.pocean.2012.06.001

Liu, Y., Weisberg, R. H., Vignudelli, S., & Mitchum, G. T. (2016). Patterns of the Loop Current system and regions of sea surface height variability in the eastern Gulf of Mexico revealed by the self-organizing maps. *Journal of Geophysical Research: Oceans*, *121*, 2347–2366. https://doi.org/10.1002/2015JC011493

Munk, W., Armi, L., Fischer, K., & Zachariasen, F. (2000). Spirals on the sea. *Proceedings of the Royal Society of London A: Mathematical, Physical and Engineering Sciences*, *456*(1997), 1217–1280. https://doi.org/10.1098/rspa.2000.0560

Parks, A. B., Shay, L. K., Johns, W. E., Martinez-Pedraja, J., & Gurgel, K. W. (2009). HF radar observations of small-scale surface current variability in the Straits of Florida. *Journal of Geophysical Research*, *114*, C08002. https://doi.org/10.1029/2008JC005025

Richardson, D. E., Llopiz, J. K., Leaman, K. D., Vertes, P. S., Muller-Karger, F. E., & Cowen, R. K. (2009). Sailfish (Istiophorus platypterus) spawning and larval environment in a Florida Current frontal eddy. *Progress in Oceanography*, *82*(4), 252–264. https://doi.org/10.1016/j.pocean.2009.07.003

Rousset, C., & Beal, L. M. (2011). On the seasonal variability of the currents in the Straits of Florida and Yucatan Channel. *Journal of Geophysical Research*, *116*, C08004. https://doi.org/10.1029/2010JC006679

Scott, R. B., Arbic, B. K., Chassignet, E. P., Coward, A. C., Maltrud, M., Merryfield, W. J., et al. (2010). Total kinetic energy in four global eddying ocean circulation models and over 5000 current meter records. *Ocean Modelling*, *32*(3-4), 157–169. https://doi.org/10.1016/j.ocemod.2010.01.005

Shay, L. K., Lee, T. N., Williams, E. J., Graber, H. C., & Rooth, C. G. (1998). Effects of low-frequency current variability on near-inertial submesoscale vortices. *Journal of Geophysical Research*, *103*(C9), 18,691–18,714. https://doi.org/10.1029/98JC01007

Shay, L. K., Parks, A. B., Haus, B. K., Martinez-Pedraja, J., Johns, W. E., Gurgel, K. W., & Cook, T. M. (2007). Resolving coastal ocean eddy activity in surface velocity signatures from Wellen Radars and an Acoustic Doppler Current Profiler. OCEANS 2007 - Europe, Aberdeen, 2007 (pp. 1-6). https://doi.org/10.1109/OCEANSE.2007.4302267

Shulzitski, K., Sponaugle, S., Hauff, M., Walter, K., D'Alessandro, E. K., & Cowen, R. K. (2015). Close encounters with eddies: oceanographic features increase growth of larval reef fishes during their journey to the reef. *Biology Letters*, *11*, 20140746. https://doi.org/10.1098/rsbl.2014.0746

Shulzitski, K., Sponaugle, S., Hauff, M., Walter, K. D., & Cowen, R. K. (2016). Encounter with mesoscale eddies enhances survival to settlement in larval coral reef fishes. *Proceedings of the National Academy of Sciences*, *113*(25), 6928–6933. https://doi.org/10.1073/pnas.1601606113

Shulzitski, K., Sponaugle, S., Hauff, M., Walter, K. D., D'Alessandro, E. K., & Cowen, R. K. (2017). Patterns in larval reef fish distributions and assemblages, with implications for local retention in mesoscale eddies. *Canadian Journal of Fisheries and Aquatic Sciences*, *75*(2), 180–192.

Sponaugle, S., Lee, T., Kourafalou, V., & Pinkard, D. (2005). Florida Current frontal eddies and the settlement of coral reef fishes. *Limnology and Oceanography*, *50*(4), 1033–1048. https://doi.org/10.4319/lo.2005.50.4.1033

Vaz, A. C., Paris, C. B., Olascoaga, M. J., Kourafalou, V. H., Kang, H., & Reed, J. K. (2016). The perfect storm: match-mismatch of bio-physical events drives larval reef fish connectivity between Pulley Ridge mesophotic reef and the Florida Keys. *Continental Shelf Research*, *125*, 136–146. https://doi.org/10.1016/j.csr.2016.06.012

Wall, C. C., Muller-Karger, F. E., Roffer, M. A., Hu, C., Yao, W., & Luther, M. E. (2008). Satellite remote sensing of surface oceanic fronts in coastal waters off west–central Florida. *Remote Sensing of Environment*, *112*(6), 2963–2976. https://doi.org/10.1016/j.rse.2008.02.007

Wang, S., Jing, Z., Liu, H., & Wu, L. (2018). Spatial and seasonal variations of submesoscale eddies in the Eastern Tropical Pacific Ocean. *Journal of Physical Oceanography*, *48*(1), 101–116. https://doi.org/10.1175/JPO-D-17-0070.1

Wang, Y., Castelao, R. M., & Yuan, Y. (2015). Seasonal variability of alongshore winds and sea surface temperature fronts in Eastern Boundary Current Systems. *Journal of Geophysical Research: Oceans*, *120*, 2385–2400. https://doi.org/10.1002/2014JC010379

Weisberg, R. H., & Liu, Y. (2017). On the Loop Current penetration into the Gulf of Mexico. *Journal of Geophysical Research: Oceans*, *122*, 9679–9694. https://doi.org/10.1002/2017JC013330

Zatsepin, A., Kubryakov, A., Aleskerova, A., Elkin, D., & Kukleva, O. (2019). Physical mechanisms of submesoscale eddies generation: Evidences from laboratory modeling and satellite data in the Black Sea. *Ocean Dynamics*, *69*(2), 253–266. https://doi.org/10.1007/s10236-018-1239-4